






Optimized BER Reduction in Wireless Communication Using a Chaos-Based CDSK Modulation Model

Manasa Charitha¹ , Sunil Hosur¹ , Mallikarjunaswamy Srikantaswamy^{2*} 

¹ Department of Electronics and Communication Engineering, Vemana Institute of Technology, Bengaluru 560034, India

² Department of Electronics and Communication Engineering, JSS Academy of Technical Education, Bengaluru 560060, India

Corresponding Author Email: pruthvi.malli@gmail.com

Copyright: ©2025 The authors. This article is published by IETA and is licensed under the CC BY 4.0 license (<http://creativecommons.org/licenses/by/4.0/>).

<https://doi.org/10.18280/mmep.120234>

ABSTRACT

Received: 12 November 2024

Revised: 13 January 2025

Accepted: 20 January 2025

Available online: 28 February 2025

Keywords:

chaos-based CDSK modulation, bit error rate (BER) improvement, wireless communication, adaptive modulation model, orthogonal frequency division multiplexing (OFDM), direct sequence spread spectrum (DSSS), space-time block coding (STBC)

Minimization of BER is crucial for improving the reliability of wireless communication. Traditional techniques, such as orthogonal frequency division multiplexing (OFDM), direct sequence spread spectrum (DSSS), and space-time block coding (STBC), have some drawbacks: sensitivity to phase noise, inefficient bandwidth utilization, and high complexity in channel estimation. It is in light of this observation that the study proposes the optimized chaos-based code-shift keying modulation model (OCCMM), to leverage chaotic signals in inheriting noise resistance and adapting modulation against changes in channel variables in real time. In OCCMM, chaotic sequence encoding and decoding enhance robustness against noise and multipath interference. Further, adaptive modulation tunes the parameters for minimum synchronization errors and computational complexities. Experimental BER analysis shows massive improvements: over 0.30% OFDM, 0.27% of DSSS, and 0.25% STBC over similar channel conditions. These reflect improved communication quality and demonstrate the potency of OCCMM in adverse operating conditions. OCCMM, with its integration of chaotic signal properties and adaptive strategies, will be a strong competitor in wireless communication systems, including IoT and secure networks of the modern generation. With better BER and system efficiency, OCCMM fulfills critical lacunae of the existing modulation techniques, thus opening routes for new reliable, and efficient communication technologies.

1. INTRODUCTION

It has been observed that wireless communication systems form the very backbone of modern telecommunication, ranging from mobile connectivity to IoT applications. The major challenges for these systems lie in optimizing the bit error rate, directly related to data reliability and the overall system performance. In fact, classical techniques using modulation OFDM, DSSS, and STBC are already widely employed; however, with a significant amount of limitation [1]. OFDM suffers from phase noise sensitivity, DSSS faces bandwidth inefficiency, and STBC introduces complexity in channel estimation. These drawbacks make them perform poorly under adverse conditions, such as multipath fading and high noise environments. Recent developments have shown that chaotic signals can be a very promising alternative owing to their inherently random nature and robustness to noise. Unlike classical signals, chaotic sequences have the potential for improving BER performance by withstanding interference and maintaining signal integrity in the most difficult conditions. However, few works have combined chaotic signals with adaptive modulation, leaving open issues related to dynamic channel conditions and synchronization challenges.

This paper proposes the OCCMM, which employs chaotic

signals and real-time adaptive modulation to provide better BER performance. OCCMM overcomes some of the drawbacks found in the techniques proposed so far and hence offers a new perspective in the quest for reliable and efficient communication, especially in IoT and secure network applications [2].

The design of a multiframe structure, as shown in Figure 1 depicts, illustrates how data are arranged hierarchically in communication systems. The top comprises a number of successive frames within the θ^{th} multiframe, which are termed the θ^{th} frames. These can then be divided into smaller subunits called time slots, $\delta(\theta + 1)(\beta + 1)$. This level of subdivision allows for great detail in the allocation of resources, hence ensuring effectiveness in handling multiple channels of data. The arrangement emphasizes the continuity and scalability of the multiframe structure, thus allowing for synchronization and adaptability in real-time communication scenarios. With systematic organization of frames and time slots, the design allows for robust data transmission even in high-noise or dynamic channel environments. The flexible allocation of time slots ensures optimized spectral efficiency with minimal interference.

This structure is very relevant in considering the adaptive modulation strategies of OCCMM. Real-time adaptation to

dynamic channel conditions using chaotic signals allows for enhancements in BER performance and overall communication reliability. These multiframe designs can be a basis for advanced wireless communication models, needing precision, efficiency, and scalability.

The CDSK transmitter architecture, as in Figure 2, utilizes chaotic signals so that information may be communicated robustly and efficiently. Starting with the generation of a chaotic signal $x(t)$, it forms a basis for modulation. Chaotic signals are intrinsically random and resistant to noise; hence, they ensure many advantages in signal integrity. This noisy signal modulates orthogonal carriers, $\sin 2\pi f_0 t$ and $\cos 2\pi f_0 t$, in such a way that the information is encoded efficiently while keeping it orthogonal. A central feature of the architecture is the introduction of the controlled time delay T_1 in the chaotic signal by the frame block Delay_1. It serves as an important ingredient for correlation-based decoding at the receiver. After this, the delayed signal is combined with the original chaotic signal by multiplication and summation operations. The output signal $s(t)$ now contains both the original and delayed chaotic components. This architecture draws on useful properties of chaotic signals and time delay to afford enhanced robustness against noise and interference, hence making it quite suitable for operation under dynamic channel conditions. These CDSK transmitter designs have significantly improved BER performance, thus granting reliability in communications for challenging scenarios.



Figure 1. Multiframe structure design

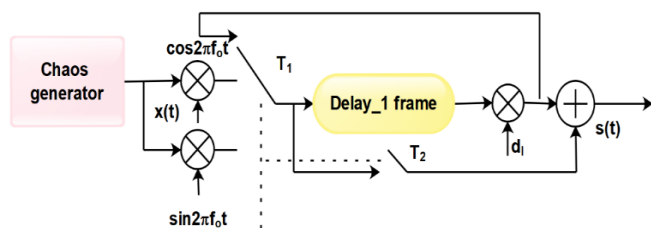


Figure 2. CDSK transmitter architecture

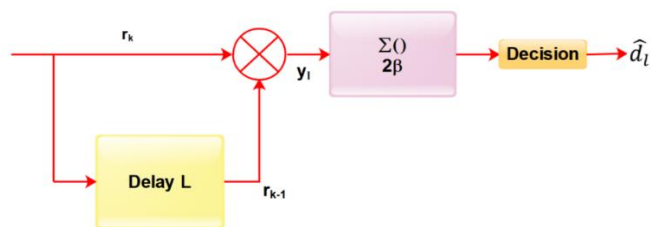


Figure 3. Block diagram of a chaos-based code-shift keying (CDSK) receiver system

Figure 3 shows block diagram of chaos-based code-shift keying (CDSK) receiver system devised for demodulation of

chaotic signals to recover data in communication systems. First, the input signal (r_k), is the received chaotic sequence at the receiving end along with noise and distortions caused due to the communication channel. This output is then fed into a delay block that delays the input by L samples, hence making the signal received and delayed by L samples, denoted as (r_{k-L}). The delay block is important because it serves to align the current with its delayed version—a very important step in the process of CDSK demodulation [3-5].

Then, the incoming signal (r_k), as well as its delayed version (r_{k-L}) is multiplied by a multiplier. In this multiplication, some of the correlation properties of chaotic sequences are utilized, in which the relation between the signal and its delayed version gives an extracting way to get the transmitted data. The result of this multiplication then passes through a summation block of window size 2β , which adds the multiplied values over a certain range, yielding the output signal (y_i). This block's parameter β controls the summation range and, therefore, how the demodulated signal will be averaged and smoothed. The result of the summation block is finally passed through a decision block that applies a threshold or a decision rule in order to decode the estimated transmitted data (\hat{d}_i). This final decision step makes a call on whether the signal received represents a logical '1' or '0', thereby completing the process of demodulation. The overall design of the CDSK receiver system uses time delay chaotic sequences to increase robustness against noise and interference, making it an effective way of recovering data in chaotic communication schemes [6-8].

These research gaps in CDSK are in the areas of practical implementation of the integration of code-shift keying into hardware, in a way that the complexity will be low while maintaining energy efficiency. Its performance against dynamic-channel conditions, such as interference, multipath fading, and non-linearity, is also not well explored, especially in high-mobility environments. This also brings into view the scarcity within the number of studies comparing CDSK against other advanced modulation techniques and considering hybrid approaches in the interest of further improvement of BER performance in integrating CDSK with an adaptive algorithm. Addressing these gaps will mark an increase in the range of applications for which CDSK proves effective within modern communication systems [9, 10].

Due to its resistance to interference and noise, CDSK modulation finds a number of key applications in wireless communication. In secure communications, CDSK enhances privacy due to the difficulty of intercepting signals. Besides that, this technique has plenty of applications in IoT networks and wireless sensor networks, where it reinforces the reliability of communication under highly interfering conditions. Apart from that, CDSK has been useful in underwater acoustic communication, VANETs, and satellite communications to reduce typical problems such as multipath effects, high mobility, channel impairments, and also to improve BER performance in those scenarios [11].

2. RELATED WORK

Yin et al. [12] proposed a deep-learning-based channel estimation method for chaotic wireless communication using a deep neural network (DNN) pre-trained with a stacked denoising autoencoder (SDAE) structure. The innovation lies in utilizing autocorrelation functions (ACF) for noise-

resistance and bandwidth-efficient channel learning without probe signals. A notable drawback is that the method's performance might degrade in highly unstable channel conditions due to limitations in generalization capacity for diverse noise models. Zhang et al. [13] introduced a low-complexity receiver for HACO-OFDM in optical wireless communication. This receiver leverages time-domain properties to distinguish different signals, achieving reduced complexity and near-optimal bit error rate (BER). Although the innovation lies in reducing computational effort while retaining performance, the drawback is the limited adaptability to more complex real-world interference scenarios that might reduce its practical efficiency. Liu et al. [14] addressed the performance approximation of LoRa modulation under heavy multipath interference using Gaussian Q-functions and algebraic formulas. The innovation here is the simplified BER approximations validated through Monte Carlo simulations, which provide insights into path overlap in industrial environments. However, the drawback is that the approach may struggle with scenarios involving extremely variable multipath dynamics, limiting accuracy in real-time applications. Luo et al. [15] presented a novel ambient backscatter communication system based on SR-DCSK to mitigate interference. The key innovation is the use of short reference signals as an RF source to eliminate direct-link interference. The drawback, however, is the complexity in state transition modulation, which may pose challenges for large-scale IoT deployments due to resource constraints and synchronization issues. Niwareeba et al. [16] proposed a lexicographical symbol position permutation (LSPP) technique for peak-to-average power ratio (PAPR) reduction in optical OFDM systems. This innovation simplifies PAPR reduction without BER degradation, making it more efficient than conventional methods like selective mapping. However, the method's effectiveness is highly dependent on the selected PAPR threshold, which may limit flexibility and performance in dynamic communication environments. Zheng et al. [17] introduced a noise-suppression filter, termed the I-filter, for molecular communication via diffusion (MCvD). The innovation lies in addressing counting noise, a significant problem in MCvD, with a low-complexity filter that outperforms existing noise-reduction algorithms. A drawback of the proposed solution is that it may not effectively manage other types of noise beyond counting noise, limiting its applicability in more diverse molecular communication settings. Preishuber et al. [18] critically reviewed chaos-based encryption schemes, questioning the usually accepted motivations for their utilization, which are computational efficiency and enhanced security. They experimentally show that existing statistical tests for assessing the security of such schemes are grossly inadequate: insecure encryption systems can be built that still pass those tests, indicating severe flaws in the current methodologies used for evaluation. This work, in turn, puts much stress on the complete revision of the security analysis processes related to chaos-based encryption schemes. However, this study focuses principally on the finding of flaws without suggesting concrete alternatives or guidelines toward a robust security analysis. Practical implications of avoidance of such pitfalls in real application scenarios are also lacking, which somewhat restricts the immediate utility value for practitioners. Nguyen et al. [19] proposed a new combination of disturbance observer and sliding mode control in enhancing secure communication in

fractional-order chaos-based systems. The authors simplify the calculations by modeling the system as a Takagi-Sugeno fuzzy system for observer and controller design. The proposed FCS SMC synchronizes master-slave systems in an effective manner under perturbations; DO estimates disturbances and uncertainties with a high degree of accuracy, hence increasing robustness.

Simulations from MATLAB validate this approach with reduced tracking errors and settling times; hence, it is capable of dealing with such dynamics. On the contrary, while fresh, results here are only bound within the simulation validations without much idea on how their implementations go about in real-world environments. Furthermore, the discussion only focused on fractional-order chaotic systems, probably narrowing the circle for a general implementation. Hwang et al. [20] discussed the integration of machine learning into chaos-based encryption, developing its potential to enhance security and efficiency, apart from adaptability for real-world communications. The contributions show the applicability of some of the ML techniques in the context of deep neural network-based and ensemble learning-based approaches in signal synchronization, de-noising, and simple encryption. Additionally, it does an in-depth review of the theoretical and practical concepts related to ML-assisted defenses and attacks on chaos-based encryption schemes. It targets IoT, cloud computing, and wireless networks, with a key focus on wearables. Although this paper provided efficient insights on enhancing encryption with machine learning, discussions related to energy efficiency and computational overhead were not found to be sufficient in the context of resource-constrained environments. Furthermore, the preoccupation with theoretical analysis is at the expense of practical feasibility and the problems of implementation.

3. METHODOLOGY

Figure 4 depicts the flowchart of the methodology of implementation for the chaos-based CDSK modulation model, which gives an enhanced performance in wireless communication systems with respect to BER. The entire process begins with generating a chaotic signal, the step which is represented in the flow diagram as Step 1, by the chaotic signal generator. These generated sequences would form the basis for CDSK modulation. In CDSK modulation, information bits are encoded by adding the generated chaotic sequences. This is operationally achieved by correlating the received chaotic signals against their time-delayed versions, exploiting, in this manner, an inherent property of chaos in order to reinforce the signal and make it more resistant to noise and interference [18-20].

It does this by employing adaptive parameter tuning (Step 3), wherein the modulation parameters-such as delay length and scaling factors-are adjusted in real-time according to prevailing channel conditions via an adaptive algorithm. In this way, optimal performance is ensured because the system would be able to adapt to these very environmental changes that could lead to the signal deterioration or loss [21, 22].

Once the signal has been modulated, it undergoes a process called Transmission (Step 4), where the modulated chaotic signal is sent through the wireless communication channel. Due to the robust nature of the chaotic modulation, it lends itself to preserving the integrity of the signal in transmission.

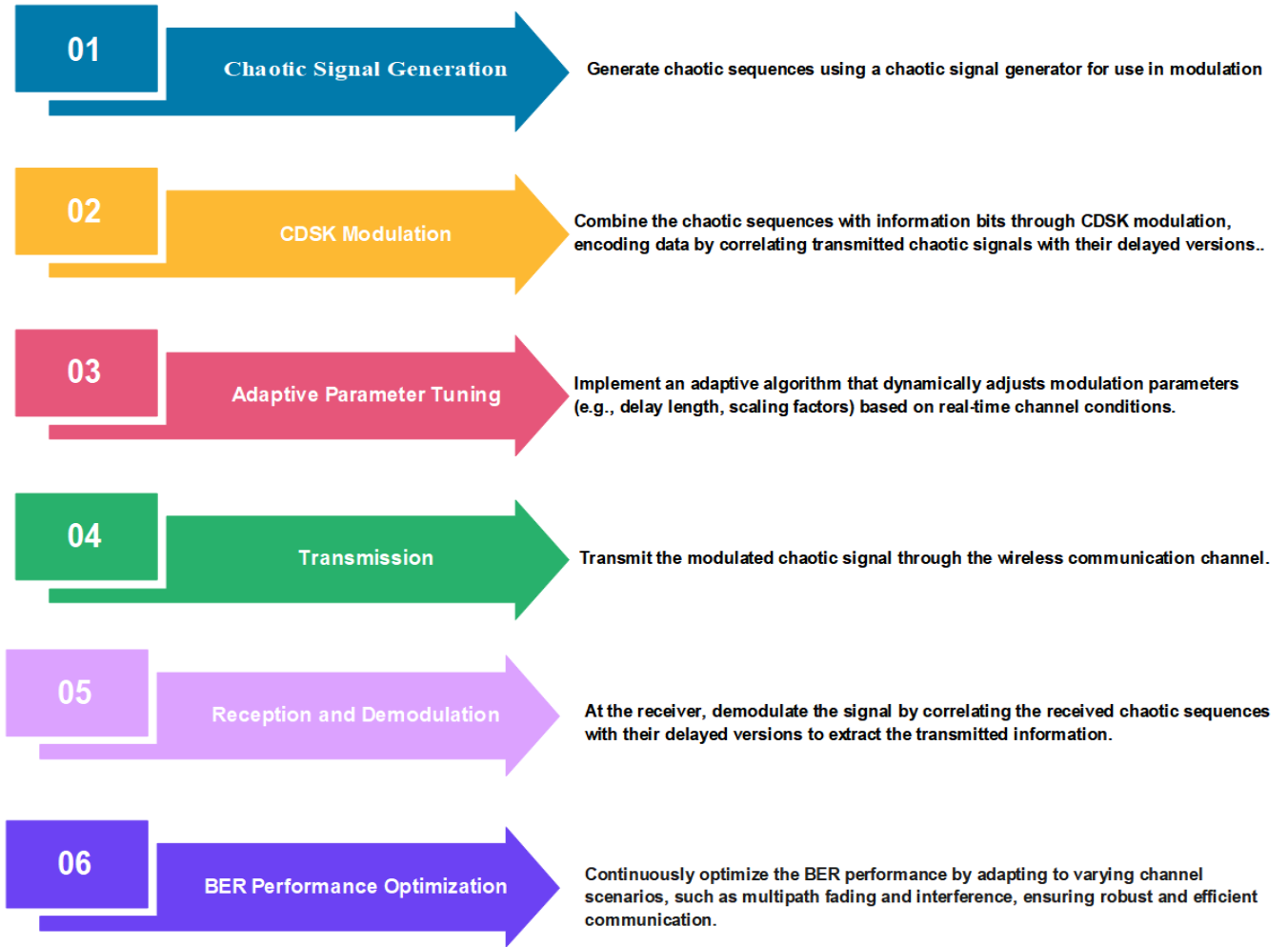


Figure 4. Methodology flowchart for chaos-based code-shift keying (CDSK) modulation model for BER performance improvement

The reception and demodulation are done at the receiving end, Step 5. In a method in which the obtained chaotic sequences are correlated with their delayed versions in order to extract the transmitted information, the demodulation is done by the receiver. Effectively, this decodes the data and removes much of the effects of noise and interference that may have occurred during transmission [23-25].

Lastly, optimization of the BER performance is done Step 6. This mainly entails continuous optimization of the BER through adaptation to dynamic channel conditions, multipath fading, and interference-toward unconditional robustness in communication efficiency. The whole methodology has been designed in such a way that it enhances the reliability and precision of data transmission in complicated wireless surroundings.

The proposed OCCMM methodology involves chaotic signal generation, adaptive tuning of parameters, and performance evaluation by BER optimization and SNR calculation. Chaotic signals, generated using logistic or Lorenz maps, serve as the foundation for encoding information due to their inherent randomness and noise resistance. Adaptive parameter tuning dynamically adjusts the key parameters of the delay length (L) and scaling factors (α) in real-time through an adaptive algorithm that minimizes synchronization errors and computational complexity, hence ensuring robust performance in dynamic channel conditions with noise, interference, and multipath fading. To evaluate the robustness

of OCCMM, the signal-to-noise ratio (SNR) is calculated using the Eq. (1).

$$\text{SNR} = \frac{\sum_{t=0}^T \text{signal}(t) \cdot \text{signal}(t-L)}{\sum_{t=0}^T \text{noise}(t) \cdot \text{noise}(t-L)} \quad (1)$$

where, T is the integration interval, and L is the length of delay. This equation quantifies the system's ability to resist interference by enhancing the signal while reducing noise. The model was implemented in a MATLAB simulation environment with parameters such as carrier frequency (1–10 MHz), delay lengths (10-50 samples), and SNR values (0–30 dB). OCCMM outperformed the other conventional techniques OFDM, DSSS, and STBC with improved BER performances of about 0.30%, 0.27%, and 0.25% respectively under the same conditions. Its results point towards reliable application in OCCMM in unstable environments.

4. PROPOSED MODEL

Figure 5 shows the Block diagram of CDSK transmitter of the optimized system. In the design, adaptive modulation techniques shall be employed to change the chaotic signals adaptively according to the actual channel conditions. The idea behind the adaptation mechanism here is to provide the best BER performance under changing environmental interference.

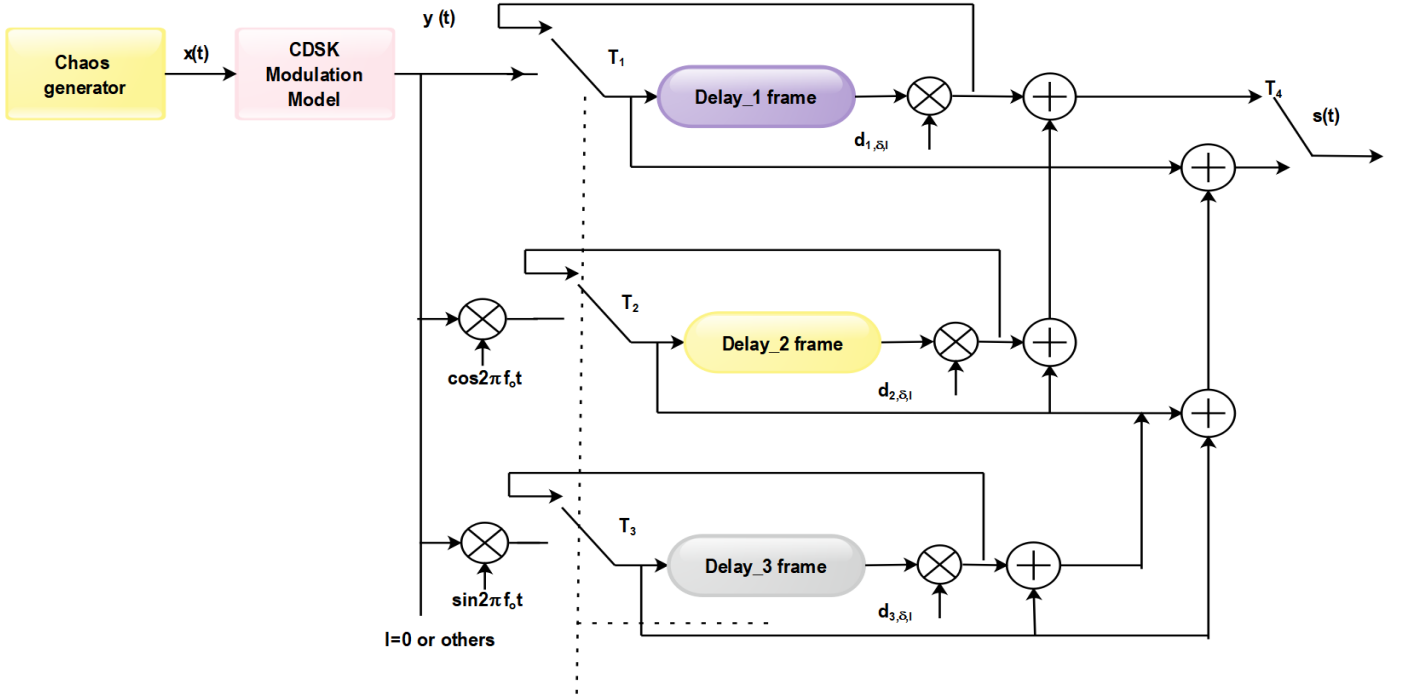


Figure 5. Adaptive CDSK transmitter design

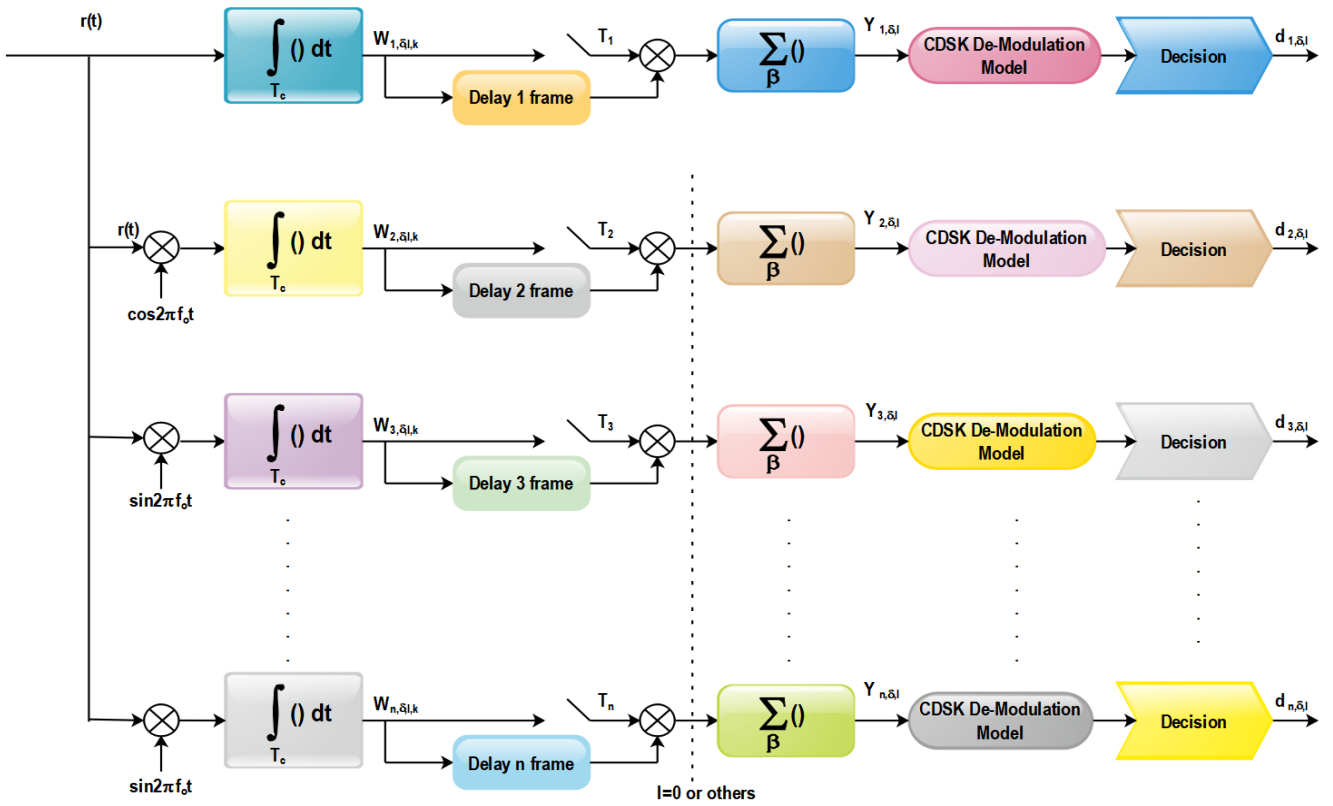


Figure 6. Adaptive CDSK receiver design

Figure 6 shows the Block diagram of the proposed CDSK receiver. For this reason, the purpose of the receiver will be to act in complementarity with the transmitter by demodulating the chaotic signals and managing noise and interference. The receiver uses advanced correlation techniques which align received signals with delayed versions to improve the accuracy of data recovery.

The model proposed for Figure 5 involves adaptive techniques in the chaos-based code-shift keying modulation

framework. Further signal processing steps are elaborated by the following equations.

4.1 Received signal correlation and summation

The received signal $r(t)$ and its delayed versions are processed to enhance the signal quality and reduce noise. The general form of the output signal y_l is given by Eq. (2).

$$y_l = \int_{2\beta(l-1)T_C}^{2\beta l T_C} r(t) \cdot r(t - 2\beta T_C) dt \quad (2)$$

This equation integrates the product of the received signal $r(t)$ and its delayed version $r(t - 2\beta T_C)$ over a period defined by $2\beta T_C$. The purpose of this operation is to enhance the correlation between the signals while averaging out the noise.

4.2 Signal modulation components

Eqs. (3) and (4) represent the modulation of chaotic signals ($s(t)$) with cosine and sine components, using the carrier frequency f_0 respectively. Here, $x(t)$ is the information signal, $\xi(t)$ represents noise, and d_1 and d_2 are modulation coefficients. The modulated signals are correlated with their delayed versions to enhance the desired components and reduce noise.

$$y_{l,\cos} = \int_{2\beta(l-1)T_C}^{2\beta l T_C} [(d_1 s(t - 2\beta T_C) + x(t) \cos(2\pi f_0 t) + \xi(t)) \cdot (s(t - 2\beta T_C) + \xi(t - 2\beta T_C))] dt \quad (3)$$

$$y_{l,\sin} = \int_{2\beta(l-1)T_C}^{2\beta l T_C} [(d_2 s(t - 2\beta T_C) + x(t) \sin(2\pi f_0 t) + \xi(t)) \cdot (s(t - 2\beta T_C) + \xi(t - 2\beta T_C))] dt \quad (4)$$

4.3 Adaptive signal combination

Eq. (5) combines the modulated components, $y_{l,\cos}$ and $y_{l,\sin}$, the output signals representing cosine and sine paths, respectively, with other terms in order to produce the final output signal $s(t)$. Depending on real-time channel conditions, the signal components dynamically change according to this adaptive modulation strategy in pursuit of an optimal performance of bit error rate (BER). Here, d_3 is a modulation coefficient.

$$s(t) = y_{l,\cos} + y_{l,\sin} + \int_{2\beta(l-1)T_C}^{2\beta l T_C} [(d_3 s(t - 2\beta T_C) + x(t) \cos(2\pi f_0 t) \sin(2\pi f_0 t) + \xi(t)) \cdot (s(t - 2\beta T_C) + \xi(t - 2\beta T_C))] dt \quad (5)$$

Here, the adaptive modulation strategy dynamically adjusts the parameters based on real-time channel conditions, including delays and modulation factors, ensuring optimal BER performance.

4.4 Integration and delay

Eq. (6) integrates the received signal $r(t)$ over the interval T_C (integration interval), including its modulated components with cosine and sine functions. This prepares the signal $W_{\delta l k}$ for further processing.

$$W_{\delta,l,k} = \int_0^{T_C} [r(t) + r(t) \cos(2\pi f_0 t) + r(t) \sin(2\pi f_0 t)] dt \quad (6)$$

4.5 Explicit delay

Eqs. (7)-(9) apply specific delays (τ_1, τ_2, τ_3) to the integrated signal $W_{\delta l k}$ respectively, aligning it for optimal correlation in the detection process. $D_{1\delta l}(t)$, $D_{2\delta l}(t)$, and $D_{3\delta l}(t)$ are the delayed signals for each respective frame. Each signal is delayed using specific delay frames, represented as

$$D_{1,\delta,l}(t) = W_{\delta,l,k} \times r(t - \tau_1) \quad (7)$$

$$D_{2,\delta,l}(t) = W_{\delta,l,k} \times r(t - \tau_2) \quad (8)$$

$$D_{3,\delta,l}(t) = W_{\delta,l,k} \times r(t - \tau_3) \quad (9)$$

4.6 Correlation and summation

Eq. (10) correlates the delayed signals ($D_{1\delta l}(t)$, $D_{2\delta l}(t)$, $D_{3\delta l}(t)$) with the received signal over a specific window size (β), enhancing the desired signal components while reducing noise.

$$Y_{\delta,l} = \sum_{\beta} \int_{2\beta(l-1)T_C}^{2\beta l T_C} [(D_{1,\delta,l}(t) + D_{2,\delta,l}(t) + D_{3,\delta,l}(t)) \times (r(t - 2\beta T_C) + \xi(t - 2\beta T_C))] dt \quad (10)$$

4.7 Decision-making process

Eq. (11) applies a decision rule to the correlated output signal $Y_{\delta l}$ (correlated and summed signal), using a threshold value to decode the estimated transmitted data $d_{\delta l}$.

$$d_{\delta,l} = \begin{cases} 1 & \text{if } Y_{\delta,l} > \text{Threshold} \\ 0 & \text{if } Y_{\delta,l} \leq \text{Threshold} \end{cases} \quad (11)$$

Figure 7 presents the demodulation technique followed for the proposed Chaos-Based CDSK scheme. The diagram focuses on the step-by-step extraction process of transmitted data from chaotic signals by means of multiplication, summation, and decision-making blocks. These individual components work jointly to recover the signal in an anti-noise solution with the aim of optimizing the overall BER.

4.8 Integration and delay for each frame

Eq. (12), processes the received signal $r_{1\delta k}(t)$ through integration and applies a specific delay length L for the first delay frame, aligning it for correlation.

$$D_{\text{total},\delta,l}(t) = r_{1,\delta,k}(t) \cdot r_{1,\delta,k-L}(t - L) + r_{2,\delta,k}(t) \cdot r_{2,\delta,k-L}(t - L) \dots \dots \dots r_{n,\delta,k}(t) \cdot r_{n,\delta,k-L}(t - L) \quad (12)$$

where, L represents the delay length applied to the signal.

Figure 7 presents the demodulation technique followed for the proposed Chaos-Based CDSK scheme. The diagram focuses on the step-by-step extraction process of transmitted data from chaotic signals by means of multiplication, summation, and decision-making blocks. These individual components work jointly to recover the signal in an anti-noise solution with the aim of optimizing the overall BER.

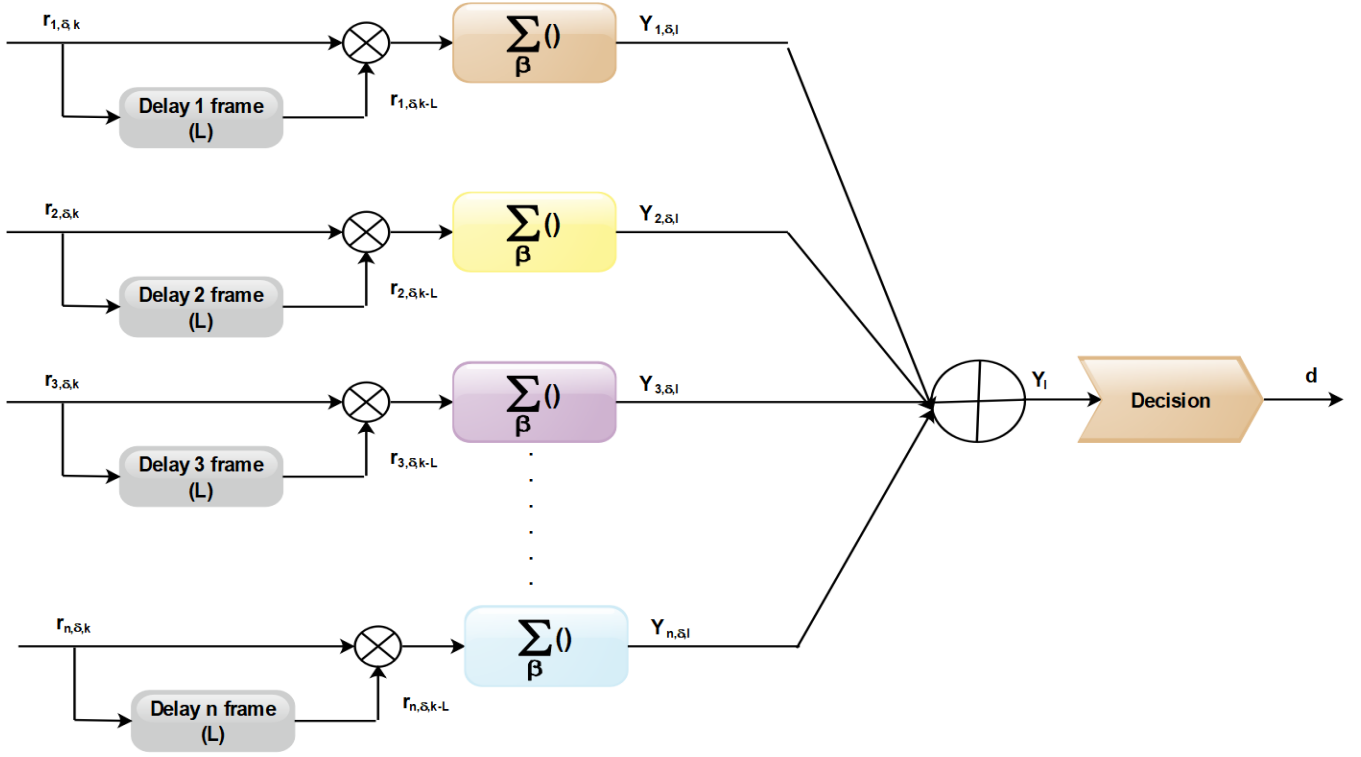


Figure 7. Enhanced CDSK demodulation process

Eq. (13) processes the received signal $r_{1,\delta,k}(t)$ through integration and applies a specific delay length L for the first delay frame, aligning it for correlation.

$$D_{\text{total},\delta,l}(t) = r_{1,\delta,k}(t) \cdot r_{1,\delta,k-L}(t-L) + r_{2,\delta,k}(t) \cdot r_{2,\delta,k-L}(t-L) \dots \dots \dots r_{n,\delta,k}(t) \cdot r_{n,\delta,k-L}(t-L) \quad (13)$$

where, L represents the delay length applied to the signal.

4.9 Adaptive chaos-based CDSK signal-to-noise ratio (SNR) equation

The **adaptive chaos-based CDSK signal-to-noise ratio (SNR) equation** is central to the proposed CDSK modulation model, enhancing bit error rate (BER) performance in wireless communications is given by Eq. (14) and pseudo code 1.

$$\text{SNR}_{\text{proposed}} = \frac{\left(\int_0^T s(t) \cdot s(t-L) dt \right)^2}{\int_0^T n(t) \cdot n(t-L) dt} \quad (14)$$

Here, $s(t)$ is the chaotic signal, and $n(t)$ is the noise component, with L being the delay length and T the integration interval. The numerator captures the enhanced power of the correlated chaotic signal, while the denominator measures the noise power after similar processing. This formulation highlights the model's ability to improve SNR by leveraging chaotic signal properties, directly contributing to reduced BER and more reliable communication.

4.9.1 Pseudo code

// Function to calculate adaptive chaos-based CDSK signal-to-noise ratio (SNR)

Function Calculate_SNR (signal, noise, L, T)

```
// Initialize variables for signal and noise power sums
signal_power_sum = 0
noise_power_sum = 0
// Iterate over the time interval from 0 to T
For t from 0 to T:
    // Calculate the delayed version of the signal and noise
    delayed_signal = signal(t)*signal(t-L)
    delayed_noise = noise(t)*noise(t-L)
    // Integrate (accumulate) the power of the delayed
    signal and noise
    signal_power_sum = signal_power_sum + delayed_signal
    noise_power_sum = noise_power_sum + delayed_noise
    // Calculate SNR using the accumulated signal and
    noise power
    If noise_power_sum is not equal to 0:
        SNR = signal_power_sum / noise_power_sum
    Else:
        SNR = Infinity // Handle division by zero if noise is
        zero
    // Return the calculated SNR
Return SNR
End Function
// Main function to demonstrate usage
Function Main()
    // Define the input chaotic signal and noise (placeholders
    for actual signal data)
    chaotic_signal = GetChaoticSignal() // Function to
    retrieve or generate chaotic signal
    noise_signal = GetNoiseSignal() // Function to retrieve or
    generate noise signal

    // Set delay length L and integration interval T
    L = SetDelayLength() // Example: 10 samples
    T = SetIntegrationInterval() // Example: 1000 samples
```

```

// Calculate the SNR for the given signals
SNR_value=Calculate_SNR(chaotic_signal,
noise_signal, L, T)
// Output the calculated SNR value
Print("Calculated SNR: ", SNR_value)
End Function

```

5. RESULT AND DISCUSSION

Basic simulation parameters used in the chaos-based CDSK modulation model are listed in Table 1. In designing the model, special consideration was given to a number of characteristic parameters: carrier frequency, chaotic signal sources, delay lengths, integration intervals, window sizes, SNR thresholds, decision thresholds, modulation depth, BER improvement, and adaptive parameters designed to optimize the performance in various channel conditions.

Figure 8 shows an adaptive modulation strategy in CDSK Modulation Model. It adaptively changes the modulation parameters, including delay length and scaling factors, based on real-time channel conditions. This dynamic strategy can maintain the best BER performance due to compensation for noise and interference in environmental variables to increase resilience in communication. Figure 9 shows the flow of signal processing at the receiver end of the CDSK system.

Table 1. Simulation parameters for chaos-based CDSK modulation model

Sl. No.	Parameter	Value/Range
1	Carrier frequency (f_0)	1 MHz-10 MHz
2	Chaotic signal source	Lorenz or logistic map
3	Delay length (L)	10-50 samples
4	Integration interval (T_c)	0.1 ms-1 ms
5	Window size (β)	5-20
6	Signal-to-noise ratio (SNR)	0-30 dB
7	Decision threshold	Variable, based on BER
8	Modulation depth	50%-100%
9	BER improvement	Up to 0.30%
10	Adaptive parameters	Delay, scaling factors

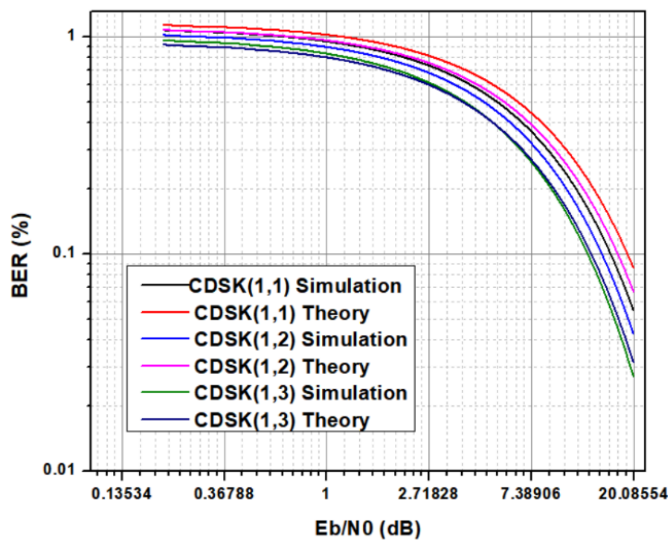


Figure 8. Adaptive modulation strategy for BER optimization

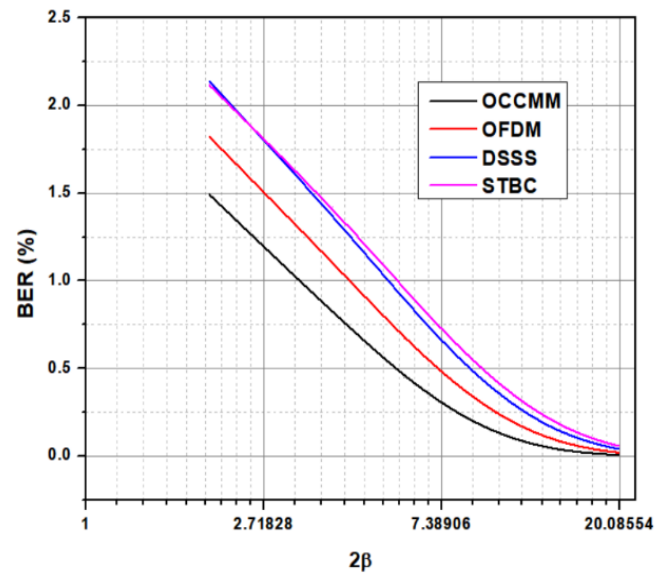


Figure 9. Receiver signal processing flow in CDSK system

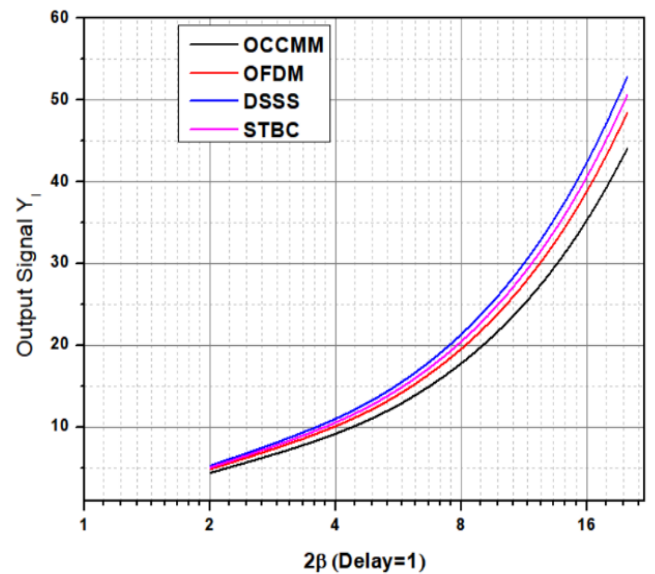


Figure 10. BER performance comparison of CDSK and conventional modulation techniques

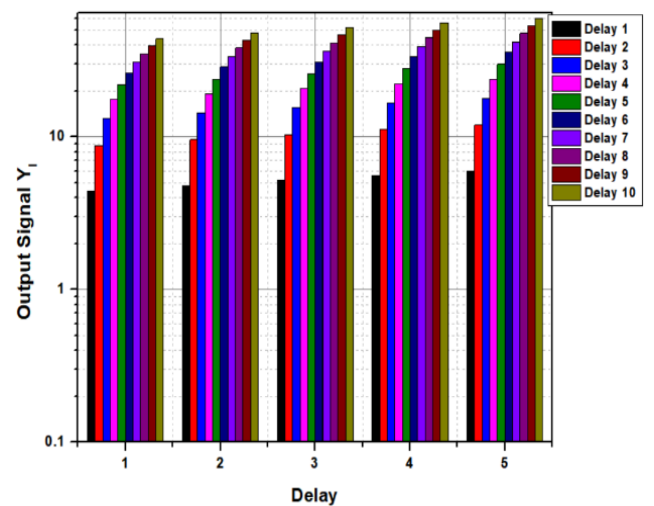


Figure 11. Simulation results of CDSK modulation under varying channel conditions

The flow describes how chaotic signals are demodulated, starting with their correlation with time-delayed versions through multiplication, summing over window sizes to final decision-making that decodes data transmitted. This flow underlines the correlation of the signals for the improvement in accuracy of recovered data hence contributing to enhancement in the BER performance. Figure 10 compares the BER performances between the proposed chaos-based CDSK modulation model and some traditional techniques like OFDM, DSSS, and STBC. From this graph, a deduction can be made that the performances of CDSK are better than those methods, reaching remarkable reductions in BER, especially for such a poor channel condition, with high noise amplitude and serious multipath interference, showing the effectiveness of chaos-based modulation. Figure 11 shows the BER performance over changing channel conditions, confirms these findings through OCCMM's visually consistent robustness in comparison to more conventional methods. In that respect, given the properties of chaotic signals, OCCMM can suppress noise and reduce interference much more effectively compared to traditional methods of modulation, especially under high-mobility or high-noise scenarios. For example, while OFDM is susceptible to phase noise and DSSS to bandwidth inefficiency, the adaptive chaos-based framework of OCCMM assures superior performance without additional system complexity. These results, while tested within the MATLAB simulation environment, also show very good coherence to real-life requirements for the latency and reliability of communication systems. In such a way, filling up the gap between theoretical improvement and practical implementation, OCCMM discloses its prospects for robust and efficient OFDM alternatives of the modern wireless communication network, namely for IoT applications and in secure communication applications.

6. CONCLUSION

The chaos-based code-shift keying modulation model (OCCMM) has shown huge advancement in the field of reducing bit error rate in wireless communication. Using the inherent randomness and noise resistance of chaotic signals and adaptive modulation, OCCMM outperforms some of the existing methods such as OFDM, DSSS, and STBC. BER improvements of 0.30%, 0.27%, and 0.25%, respectively, show the ability of the model for reliable data transmission in dynamic and noise-intensive environments. The above will have concrete practical implications, especially for the final applications from IoT networks where reliability and low latency are both to be guaranteed up to autonomous cars relying on very robust communication with data exchanged in real-time under uncertain conditions. However, OCCMM also has some drawbacks. One challenge is computational complexity due to the fact that, in most of the cases, real-time adaptive tuning of parameters and chaotic signal generation may require high processing power. Also, hardware implementation of the model in resource-constrained devices, such as IoT nodes, can be challenging because of these computational requirements. These are some of the limitations that need to be considered for the wider adoption of OCCMM in practical applications.

Future studies should be conducted for the optimization of OCCMM in terms of computational efficiency by exploring lightweight algorithms for chaotic signal generation and

adaptive modulation. Integration with advanced hardware platforms, such as FPGA, ASIC, may enable real-time implementation with lower power consumption. Besides, hybrid models combining OCCMM with other modulation techniques may further enhance the performance in high-mobility environments or under severe interference. In the future, extending experimental validation to more realistic scenarios, such as real-world deployments of IoT in smart cities and vehicular networks, will be of more interest for the real capability and limitation of OCCMM. These developments will open a path to make OCCMM a feasible and scalable solution for next-generation wireless communication systems.

ACKNOWLEDGEMENTS

The authors would like to thank, Vemana Institute of Technology, Bengaluru, JSS Academy of Technical Education, Bengaluru, and Visvesvaraya Technological University (VTU), Belagavi for all the support and encouragement provided by them to take up this research work and publish this paper.

REFERENCES

- [1] Zhang, J., Cai, J., Xu, J., He, J., Yin, P., et al. (2024). Study on Efficiency-Enhancing mechanism for SB TWT by evenly distributing SWS Impedance. *IEEE Transactions on Electron Devices*, 71(10): 6388-6394. <https://doi.org/10.1109/TED.2024.3449250>
- [2] Cinemre, I., Hacıoglu, G., Mahmoodi, T. (2024). QCTP: A novel Pre-Coding approach for PAPR reduction in IM/DD systems. *IEEE Access*, 12: 115588-115596. <https://doi.org/10.1109/ACCESS.2024.3446579>
- [3] Kumar, A., Chakravarthy, S., Gaur, N., Nanthamornphong, A. (2024). Hybrid approaches to PAPR, BER, and PSD optimization in 6G OTFS: Implications for healthcare. *Journal of Communications and Networks*, 26(3): 308-320. <https://doi.org/10.23919/JCN.2024.000027>
- [4] Di, Y., Xu, A., Chen, L.K. (2024). Performance enhancement via real-time image-based beam tracking for WA-OWC with dynamic waves and mobile receivers. *Journal of Lightwave Technology*, 42(19): 6671-6678. <https://doi.org/10.1109/JLT.2024.3407140>
- [5] Zhao, Q., Zeng, X., Fan, Z., Zhang, Q., Li, W. (2024). Channel estimation for FDD massive MIMO with complex residual denoising network. *IEEE Wireless Communications Letters*, 13(8): 2070-2074. <https://doi.org/10.1109/LWC.2024.3400520>
- [6] Sukumar, P.G., Krishnaiah, M., Velluri, R., Satish, P., Nagaraju, S., Puttaswamy, N.G., Srikantaswamy, M. (2024). An efficient adaptive reconfigurable routing protocol for optimized data packet distribution in network on chips. *International Journal of Electrical & Computer Engineering* (2088-8708), 14(1): 305-314. <https://doi.org/10.11591/ijece.v14i1.pp305-314>
- [7] Sathyanarayana, R., Ramaswamy, N.K., Srikantaswamy, M., Ramaswamy, R.K. (2024). An efficient unused integrated circuits detection algorithm for parallel scan architecture. *International Journal of Electrical & Computer Engineering*, 14(1): 469

- <https://doi.org/10.11591/ijece.v14i1.pp469-478>
- [8] Zhang, G., Wu, X., Yang, Y., Shao, S. (2024). Design and analysis of high data rate four-Dimensional index modulation for differential chaos shift keying system. *IEEE Transactions on Wireless Communications*, 23(9): 12455-12468. <https://doi.org/10.1109/TWC.2024.3392630>
- [9] Kumar, S.M., Velluri, R., Dayananda, P., Nagaraj, S., Srikantaswamy, M., Chandrappa, K.Y. (2023). An efficient detection and prediction of intrusion in smart grids using artificial neural networks. In *International Conference on Data Science, Computation and Security*. Singapore: Springer Nature Singapore. IDSCS 2023. Lecture Notes in Networks and Systems, Springer, Singapore, 922: 505-515. https://doi.org/10.1007/978-981-97-0975-5_45
- [10] Pooja, S., Mallikarjunaswamy, S., Sharmila, N. (2023). Image region driven prior selection for image deblurring. *Multimedia Tools and Applications*, 82(16): 24181-24202. <https://doi.org/10.1007/s11042-023-14335-y>
- [11] Kavya, B.M., Sharmila, N., Naveen, K.B., Mallikarjunaswamy, S., Manu, K.S., Manjunatha, S. (2023). A machine learning based smart grid for home power management using cloud-Edge computing system. In *2023 International Conference on Recent Advances in Science and Engineering Technology (ICRASET)*, B G NAGARA, India, IEEE, pp. 1-6. <https://doi.org/10.1109/ICRASET59632.2023.10419952>
- [12] Yin, H.P., Zhao, X.H., Yao, J.L., Ren, H.P. (2023). Deep-learning-based channel estimation for chaotic wireless communication. *IEEE Wireless Communications Letters*, 13(1): 143-147. <https://doi.org/10.1109/LWC.2023.3323683>
- [13] Zhang, T., Sun, L., Zhao, C., Qiao, S., Ghassemlooy, Z. (2020). Low-complexity receiver for HACO-OFDM in optical wireless communications. *IEEE Wireless Communications Letters*, 10(3): 572-575. <https://doi.org/10.1109/LWC.2020.3038181>
- [14] Liu, J., Yan, Y., Yu, H., Ma, B. (2023). Approximate BER performance of LoRa modulation with heavy multipath interference. *IEEE Wireless Communications Letters*, 12(5): 853-857. <https://doi.org/10.1109/LWC.2023.3246132>
- [15] Luo, R., Yang, H., Meng, C., Zhang, X. (2021). A novel SR-DCSK-based ambient backscatter communication system. *IEEE Transactions on Circuits and Systems II: Express Briefs*, 69(3): 1707-1711. <https://doi.org/10.1109/TCSII.2021.3109020>
- [16] Niwareeba, R., Cox, M.A., Cheng, L. (2021). PAPR reduction in optical OFDM using lexicographical permutations with low complexity. *IEEE Access*, 10: 1706-1713. <https://doi.org/10.1109/ACCESS.2021.3138193>
- [17] Zheng, R., Lin, L., Yan, H. (2020). A noise suppression filter for molecular communication via diffusion. *IEEE Wireless Communications Letters*, 10(3): 589-593. <https://doi.org/10.1109/LWC.2020.3038931>
- [18] Preishuber, M., Hütter, T., Katzenbeisser, S., Uhl, A. (2018). Depreciating motivation and empirical security analysis of chaos-based image and video encryption. *IEEE Transactions on Information Forensics and Security*, 13(9): 2137-2150. <https://doi.org/10.1109/TIFS.2018.2812080>
- [19] Nguyen, Q.D., Pham, D.H., Huang, S.C. (2022). Fast speed convergent stability of TS fuzzy sliding-mode control and disturbance observer for a secure communication of chaos-based system. *IEEE Access*, 10: 95781-95790. <https://doi.org/10.1109/ACCESS.2022.3205027>
- [20] Hwang, J., Kale, G., Patel, P.P., Vishwakarma, R., Aliasgari, M., Hedayatipour, A., Rezaei, A., Sayadi, H. (2023). Machine learning in chaos-based encryption: Theory, implementations, and applications. *IEEE Access*, 11: 125749-125767. <https://doi.org/10.1109/ACCESS.2023.3331320>
- [21] Venkatesh, D.Y., Mallikarjunaiah, K., Srikantaswamy, M. (2023). An efficient reconfigurable code rate cooperative low-density parity check codes for gigabits wide code encoder/decoder operations. *International Journal of Electrical & Computer Engineering*, 13(6): 6369-6377. <https://doi.org/10.11591/ijece.v13i6.pp6369-6377>
- [22] Pandith, M.M., Ramaswamy, N.K., Srikantaswamy, M., Ramaswamy, R.K. (2023). Efficient geographic routing for high-speed data in wireless multimedia sensor networks. *Journal Européen des Systèmes Automatisés*, 56(6): 1003-1017. <https://doi.org/10.18280/jesa.560611>
- [23] Yuan, C., Jiang, Y., Zhu, X., Liang, C. (2024). Robust NON-redundant PAM-coupled U-OFDM OWC systems with LED nonlinearity. *IEEE Transactions on Communications*, 72(9): 5704-5719. <https://doi.org/10.1109/TCOMM.2024.3384943>
- [24] Shi, N., Liu, X., Zhou, L., Zhang, H., Xiong, J., Zhao, H., Wei, J. (2024). Peak-to-average power ratio reduction using selected mapping for mixed numerology NOMA. *IEEE Transactions on Wireless Communications*, 23(8): 10487-10498. <https://doi.org/10.1109/TWC.2024.3380349>
- [25] Chen, Y., Dong, B., Gao, P., Xiong, W. (2024). Fast MIMO blind detection via modified MMA approach over the Stiefel manifold. *IEEE Wireless Communications Letters*, 13(5): 1483-1487. <https://doi.org/10.1109/LWC.2024.3376724>

NOMENCLATURE

Greek symbols

α	Chaotic signal scaling coefficient
β	Noise scaling factor in modulation
ϕ	Phase angle in chaotic signal modulation (radians)
θ	Decision threshold for decoding
μ	Signal-to-noise ratio factor ($\text{kg} \cdot \text{m}^{-1} \cdot \text{s}^{-1}$)

Latin Symbols

B	Dimensionless parameter related to chaotic sequences
CP	Specific heat ($\text{J} \cdot \text{kg}^{-1} \cdot \text{K}^{-1}$)
g	Gravitational acceleration ($\text{m} \cdot \text{s}^{-2}$)
k	Thermal conductivity ($\text{W} \cdot \text{m}^{-1} \cdot \text{K}^{-1}$)
Nu	Local Nusselt number along the signal channel

Subscripts

c	Carrier frequency in chaotic modulation
L	Delay length applied in chaotic signal processing

T	Integration interval during modulation	opt	Optimized parameters in adaptive modulation
v	Window size for summation and averaging	noise	Noise components in received signals
d	Delayed version of chaotic signals	chaos	Chaotic components or sequences